

CdS NANOCRYSTALLINE STRUCTURED GROWN ON POROUS SILICON SUBSTRATES VIA CHEMICAL BATH DEPOSITION METHOD

M. A. MAHDI^{a,b,*}, ASMIET RAMIZY^a, Z. HASSAN^a, S. S. NG^a, J. J. HASSAN^{a,b}, S. J. KASIM^b

^a*Nano-Optoelectronics Research and Technology Laboratory (N.O.R)
School of Physics, University Sains Malaysia, 11800 Penang, Malaysia*

^b*Physics Department, College of Science, Basra University, Basra, Iraq*

Cadmium sulfide (CdS) nanoflowers, nanoplates and nanofire structures were synthesized by chemical bath deposition (CBD) on porous silicon (PS). The PS substrates were prepared by electrochemical etching method using alternating current (ACPS) and direct current (DCPS). Scanning electron microscopy (SEM) revealed that the CdS fabricated on ACPS had two nanostructures, nanoflowers and nanoplates while the CdS on DCPS showed a novel structure named nanofire. X-ray diffraction patterns showed that the CdS nanocrystalline structured in wurtzite (hexagonal) phase. Photoluminescence (PL) of CdS nanoflowers and nanoplates structures showed a high intensity with blue-shift compared with nanofire structure. Furthermore, Raman spectra of CdS nanostructures showed red shift of peaks positions.

(Received December 5, 2011; Accepted January 11, 2012)

Keywords: Nanostructure CdS, Chemical Bath Deposition, Porous Silicon.

1. Introduction

Cadmium sulfide (CdS) is one of the most important II–VI semiconductors, with a direct bulk band gap of 2.42 eV at room temperature, and is extensively used for electro-optics devices; enhance the detection of gas and optical sensing of other materials [1-6]. Furthermore, CdS can be synthesized as a variety of nanostructures, including nanoparticles, nanorods, nanowires, nanosheets, nanoplates, nanowalls and nanoflowers using various techniques [7-12]. Among these methods, CBD method offers a simple and inexpensive route to deposit homogeneous and high quality thin films and has been widely used to synthesize nanocrystalline semiconductor thin films [13-16]. In CBD method, the structure and morphology of the product is influenced by factors such as supersaturation, nucleation and growth rates, colloidal stability, recrystallization, and the aging process [17]. The morphology of deposited layer strongly depends on the nature of the substrate surface, this feature is widely used by researchers to obtain the desired structures, i.e., porous substrates like an anodic aluminum oxide (AAO) template to synthesize CdS nanowires [18,19].

The objective of this work is to synthesize nanocrystalline CdS structures and study the effect of the substrate surface on the morphology of the grown layers. Also the Photoluminescence (PL) and Raman spectra of the prepared samples were analyzed.

2. Experimental details

P-type Si(111) was used to fabricate PS using an electrochemical etching method.[20] To prepare ACPS, an AC current density of 35 mA/cm was applied while a 40 mA/cm² current density was used to prepare DCPS at room temperature. In a typical experiment, 0.05M of CdCl₂

*Corresponding author: mazinauny74@yahoo.com

was dissolved in 100 ml distilled water (DI) and 0.1M thiourea was added dropwise with continuous stirring for 10 minutes. The pH of solution was fixed at 11 by adding ammonia NH_3 . The solution was transferred to another beaker where the PS substrates were fixed onto glass slides and tilted at 45° . The temperature was gradually raised to 90°C . Total deposition time was 2h. The samples were removed from the solution, washed in hot DI, and dried naturally. The morphology of the nanostructures was characterized using scanning electron microscope (SEM). X-Ray diffraction (XRD, PANalytical X'Pert PRO with $\text{CuK}\alpha$ radiation) was employed to determine the crystalline structure of nanocrystalline CdS. PL and Raman spectroscopy were carried out at room temperature using a Jobine Yvon HR 800 UV system with excitation wavelengths of 325 nm and 554 nm, respectively.

3. Results and discussion

3.1 Morphology

Fig. 1 (A and B) shows the SEM images of PS prepared by AC (ACPS) and DC (DCPS) currents, respectively. ACPS has a different pore shape and concentration than DCPS, with most pores shaped like a human heart with sharp edges in contrast to circles of various diameters. Fig. 1 C and D shows the CdS nanoflowers and nanoplates on ACPS at different magnifications. The CdS nanoflowers and nanoplates structures were grown on a large area of ACPS substrate. The heterogeneous pore shape and distribution lead to different nucleation centers of CdS nanoparticles, which may cause the formation of different structures on the substrate surface such as flowers and plates. CdS grown on DCPS had another shape like fire [21] (see Fig.1 G), which we named nanofire (see Fig.1 E, F and G). Nanofire structure may be formed when air bubbles contained in holes in the PS substrate come out upon immersion in an electrolyte solution and takes the pore's shape. The EDS of CdS nanocrystalline prepared on ACPS and DCPS showed that the Cd/S ratio was of 1.6 and 1.65, respectively.

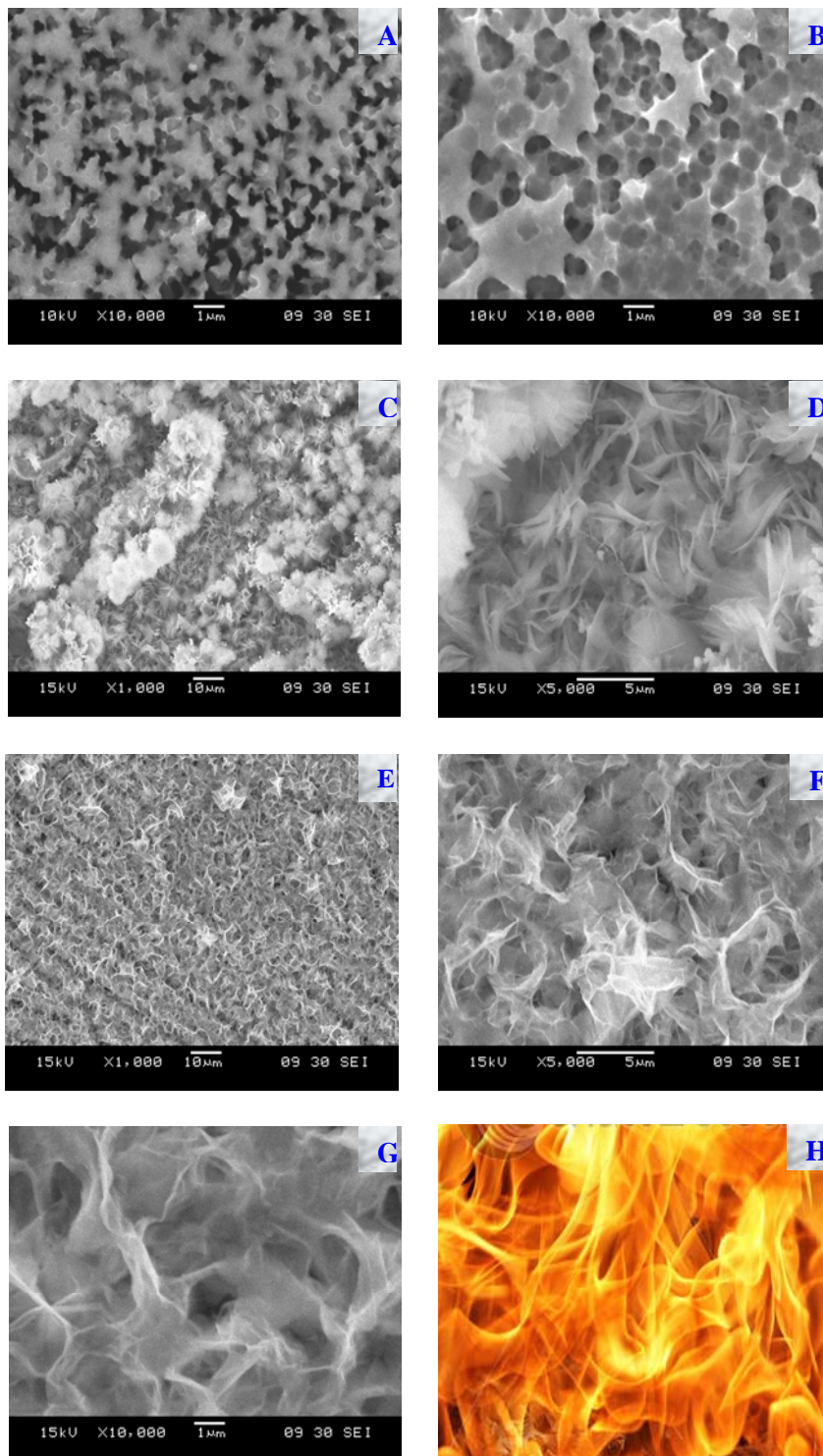


Fig.1: SEM images of (A) ACPS, (B) DCPS, (C), (D), CdS nanoflowers and nanoplates on ACPS, (E) and (F) and (G) CdS nanofire structure on DCPS, (H) fire image[21].

3.2 Crystalline structure

Fig.2 shows the XRD pattern of the CdS nanocrystalline structured grown on ACPS and DCPS substrates. The patterns contain several diffraction peaks corresponds to wurtzite (hexagonal) phase of CdS according to the standard database (ICCD, PDF-4, 00-001-0783). The lattice constants a and c of the unit cell can be calculated using the following relation:

$$\frac{1}{(d_{hkl})^2} = \frac{4}{3} \left(\frac{h^2 + hk + k^2}{a^2} \right) + \frac{l^2}{c^2}, \quad (1)$$

Where d is the interplanar spacing of the atomic planes, h, k, l are Miller indices.

The lattice parameters a and c values were 6.69 and 4.10 \AA for CdS nanoflower structured grown on ACPS substrate while it were 6.67 and 4.13 \AA for CdS nanofire structure on DCPS. The (c/a) was 1.61 and 1.63 for nanoflower and nanofire respectively, and comparing with standard data ($c/a=1.62$), the two samples seemed effected by stress and strain.

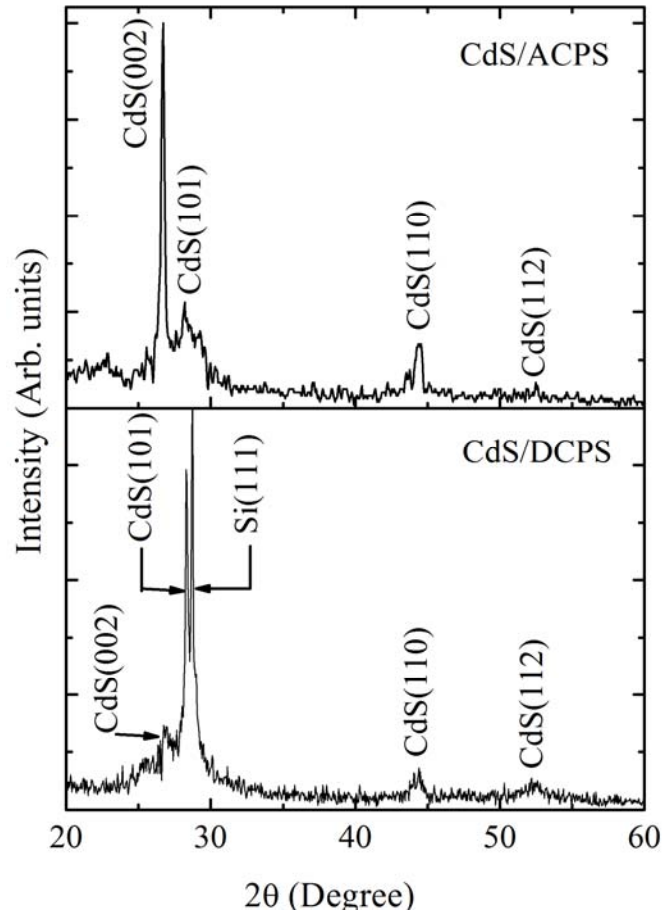


Fig.2: XRD patterns of CdS nanoflowers grown on ACPS and CdS nanofire grown on DCPS

3.3 Photoluminescence spectra

Fig. 3 shows the PL spectra of CdS nanocrystalline structures samples prepared on ACPS and DCPS substrates. For CdS nanoflowers and nanoplates, the PL emission peak appeared at 493

nm, known as green emission band of CdS. In nanocrystalline structures, the quantum confinement of photons occurs. Thus, the emission peak normally shifts towards shorter wavelengths by the same amount as the shift of the direct inter-band transition energy [22]. Therefore, the emission peak of the CdS nanoflowers and nanoplates was blue-shifted. CdS on ACPS showed another high intensity emission peak at 510 nm, which could be due to the sample having more than one nanostructure such as nanoflowers and nanoplates, each of which has its own optical band gap. Ordinarily, two emissions can be obtained from nanocrystalline semiconductor: a sharp excitonic emission near the absorption edge and another broad emission at a longer wavelength due to surface states or defects [23]. This high intensity emission could be due to band-to-band recombination and the appearance of other emission peaks at 590, 610 and 650 nm can be attributed to surface defects that act as radiative or nonradiative centers or sulfur vacancies [24]. The CdS nanofire structure showed a PL peak at 512 nm that is red shifted compared with the nanoflowers structure, which means that the optical band gap is increased. The major difference in the intensity of PL peaks can be attributed to the difference in CdS nanostructures shape and the broadening in emission peaks can be attributed to heterogeneity in the size and shape of the nanostructured [25]. In addition, the emergence of emission peaks in the range of 600 – 700 nm can be attributed to porous silicon, which increases its optical band gap to the visible region of the optical spectrum [26].

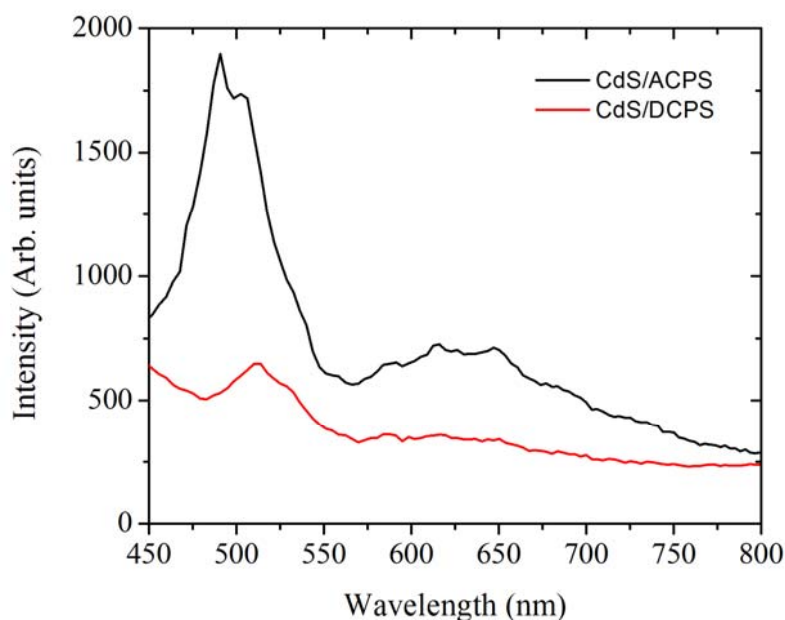


Fig.3: Room temperature PL spectra of CdS nanocrystalline structures on ACPS and DCPS substrates.

3.4 Raman analysis

Fig. 4 displays the Raman spectra of the prepared CdS nanocrystalline structures. Three peaks are observed in the two samples. The peak at 519 cm^{-1} is related to porous Si and was red shifted by 3 cm^{-1} from the bulk Si peak [27]. The other peaks correspond to the first and second order longitudinal optical (LO) phonon modes of the CdS nanocrystalline structures. Bulk CdS fundamental (1LO) and overtone (2LO) modes are detected at 305 cm^{-1} and near 605 cm^{-1} , respectively [28]. Raman peaks positions of CdS nanoflowers and nanoplates structures of 1LO and 2LO were red shifted to around 300 cm^{-1} and 599 cm^{-1} , respectively, while the nanofire structure had peaks at 297 and 595 cm^{-1} . The red shift in the Raman peaks positions was due to the phonon confinement effect. In semiconductor materials, the strength of exciton-phonon coupling can be assessed by the intensity ratio of overtone of phonon to fundamental (I_{2LO}/I_{1LO}). [29] The intensity ratio of the nanofire structure was 1.02. When compared to 0.74 for the other samples, it

is clear that the strength of exciton-LO phonon coupling in a nanofire structure is stronger than in nanoflowers. Thus, the 2D structure of nanofire showed a greater effect of phonon confinement.

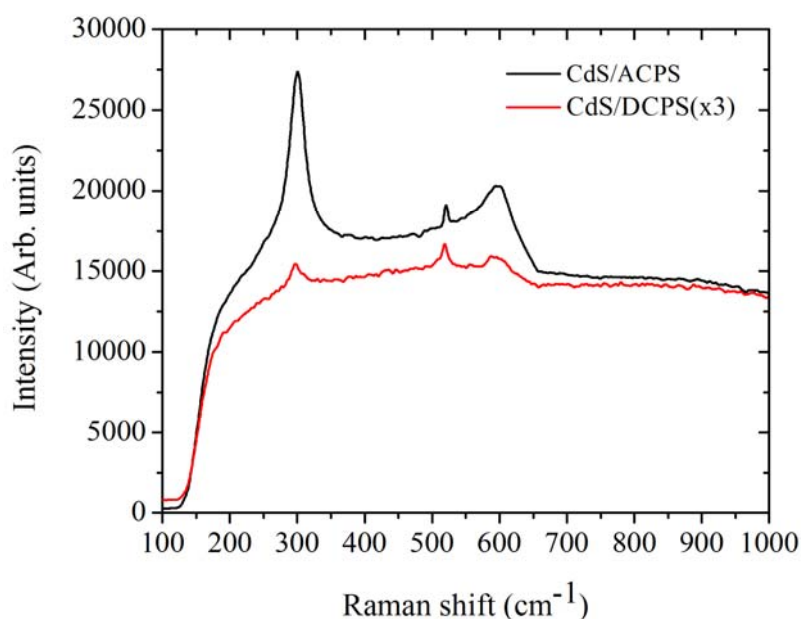


Fig. 4: Raman spectra of CdS nanocrystalline structures prepared on ACPS and DCPS

4. Conclusions

Porous silicon substrates were prepared using an electrochemical etching method. CdS nanoflowers, nanoplates and nanofire structures were synthesized on porous silicon by CBD method. The shape and pores concentration of substrates influenced the CdS nanostructures formation. The CdS on ACPS showed two nanostructures, nanoflowers and nanoplates and formed a novel structure named nanofire on DCPS. The PL spectra of the CdS nanoflowers and nanoplates structures showed two blue shifted emission peaks compared with the bulk structure of CdS. The appearance of two emission peaks was due to the types of structure in the sample, including nanoflowers and nanoplates, and the energy gap for each structure is different. The CdS nanofire structure showed a low intensity emission peak closer to the bulk CdS absorption edge compared with the other sample. All CdS nanocrystalline structures showed red shift in the Raman spectra.

Acknowledgment

Support from research university (FGRS) grant and University Sains Malaysia is gratefully acknowledged.

References

- [1] H. Murai, T. Abe, J. Matsuda, H. Sato, S. Chiba, Y. Kashiwaba, *Appl. Surf. Sci.* **244**, 351 (2005)
- [2] F. L. Castillo-Alvarado, J. A. Inoue-Chávez, O. Vigil-Galán, E. Sánchez-Meza, E. López-Chávez, G. Contreras-Puente, *Thin Solid Films*, **518**, 1796 (2010).
- [3] A. Rios-Flores, J. L. Pena, V. Castro-Pena, O. Ares, R. Castro-Rodríguez, A. Bosio, *Sol. Energy*, **84**, 1020 (2010).

- [4] J. Han, C. Spanheimer, G. Haind, G. Fu , V. Krishnakumar , J. Schaffner , C. Fan, KuiZhao, A. Klein, W. Jaegermann, *Sol. Energ. Mat. Sol. C* **95**, 816 (2011)
- [5] J. Zhai, D. Wang, L. Peng, Y. Lin, X. Li and T. Xiea, *Sensor. Actuator. B* **147**, 234 (2010)
- [6] Y. Kang, D. Kim, *Sensor. Actuator. A*, 125,114 (2006)
- [7] J. Baraman, K.C.Sarm, M. Sarm, K. Sarm, *Indian J. Pure Appl. Phys.* 46,339 (2008)
- [8] L. Zahng, D. Qin, *Chalcoge. Lett.* 8, 349 (2011)
- [9] J. S. Jang, U. A. Joshi, J. S. Lee, *J. Phys. Chem. C* 111, 13280 (2007)
- [10] F. Chen, R. Zhou. L. Yang, M. Shi, G. Wu, M. Wang, H. Chen, *J. Phys. Chem. C* **112**, 134557 (2008)
- [11] S. A. Vanalakar, S.S. Mali, R.C. Pawar, N. L. Tarwal, A.V. Moholkar, J. A. Kim, Y. Kwon, J. H. Kim, P.S. Patil, *Electrochimica Acta.* **56**, 2762 (2011)
- [12] J. K. Dongre, M. Ramrakhiani, *J. Alloys Compd.* **487**, 653 (2009)
- [13] F. A Pizzarello, *J. Appl. Physics* **35**, 2730 (2009)
- [14] M. A. Mahdi, S. J. Kasem, J. J. Hassen1, A. A. Swadi, S. K. J. Al-Ani, *Int. J. Nanoelec. Mater.* **2**, 41 (2009)
- [15] V. B. Sana, B. H. Pawar, *Chalcoge. Lett.* 6, 415 (2009)
- [16] S. Prabahar, M. Dhanam, *J. Cryst. Growth* 285,41 (2005)
- [17] C. C. Koch, *Nanostructured Materials, Processing, Properties and Potential, Applications*, William Andrew Publishing, Norwich, New York, U.S.A. (2002)
- [18] Y. Yang, H. Chen, Y. Mei, J. Chena, X. Wu, X. Bao, *Solid State Commun.* **123**,279 (2002)
- [19] F. Han, G. Meng, X. Zhao, Q. Xu, J. Liu, B. Chen, X. Zhu, M. Kong, *Mater. Lett.* **63**,2249 (2009)
- [20] A. Ramizy, Z. Hassan, K. Omar, *Mater. Lett.* **65**,61 (2011)
- [21] <http://www.shutterstock.com/pic.mhtml?id=13998838>
- [22] K. Vishwakarma, O.P. Vishwakarma, *Int. J. Nanotech. and Appl.* **4**,13 (2010)
- [23] G. Tai and W. Gue, *Ultrason. Sonochem.* **15**,350 (2008)
- [24] M. Karimi, M. Rabiee, F. Moztaezadeh, M. Bodaghi, M. Tahriri, *Solid State Commun.* **149**, 1765(2009)
- [25] A. Ramizy, Z. Hassan, K. Omar, Y. Al-Douri, M. A. Mahdi, *Appl. Surf. Sci.* **257**,6112 (2011)
- [26] H. M. Fan, X. F. Fan, Z. H. Ni, Z. X. Shen, Y. P. Feng, B. S. Zou, *J. Phys. Chem. C* **112**,1865 (2008)
- [27] A. Ramizy, Z. Hassan, K. Omar, *Sci. China Tech. Sci.* **4**,58 (2011)
- [28] M. Abdulkbadar, B. Thomas, *Nanostruc. Mater.* **5**, 289 (1995)
- [29] A. Pan, R. Liu, Q. Yang, Y. Zhu, G. Yang, B. Zou, K. Chen, *J. Phys. Chem. B* **109**, 24268 (2005)